Spectral hole burning and gain saturation in short-cavity semiconductor lasers

K. Henneberger and F. Herzel
Institut für Physik, Universität Rostock, Aussenstelle Güstrow, Goldberger Strasse 12, O-2600 Güstrow, Germany

S. W. Koch, R. Binder, A. E. Paul, and D. Scott
Optical Sciences Center and Physics Department, University of Arizona, Tucson, Arizona 85721
(Received 24 June 1991)

A coupled set of equations for carrier distributions and stimulated emission in a semiconductor laser is presented, based on a nonequilibrium Green's-function formulation. Carrier momentum-dependent dephasing caused by carrier-carrier scattering and frequency-dependent optical gain are shown to govern the interplay between carrier relaxation and stimulated recombination. Ignoring the interband Coulomb interaction, the coupled system of equations for the carrier distribution functions and the optical gain is solved self-consistently for a single-mode short-cavity semiconductor laser under steady-state operation conditions. Numerical results show spectral and kinetic hole burning as well as nonlinear gain saturation.

PACS number(s): 42.55.Px, 42.65.−k

I. INTRODUCTION

The problem of spectral hole burning and gain saturation in semiconductor lasers is not only central for the understanding of the laser operation, but it also provides detailed insight into the dynamics of the coupled carrier-photon system. A consistent theoretical analysis requires a unified treatment of light field and carrier dynamics, including the fundamental relaxation and dephasing mechanisms. For example, the dynamic evolution of the carrier distributions in semiconductor lasers is generally governed by the interplay between the nonresonant incoherent pumping (carrier injection), the relaxation of the injected carriers, and the interband recombination by spontaneous and stimulated light emission.

Substantial work on semiconductor lasers has been published over the past two decades [1–3]. Particularly relevant for our present study is the theoretical analysis by Korenman [4] and by Zée [5], where the broadening mechanisms in semiconductor lasers are included as phenomenological parameters. Experimental investigations of gain saturation and spectral hole burning in cw semiconductor lasers have been reported [1–3,6–8] and femtosecond time-resolved investigations on semiconductor amplifiers are presented in Ref. [9].

In this paper we investigate nonlinear saturation and spectral hole burning for the case of short-cavity bulk semiconductor lasers, where only single-mode operation is possible. We present a self-consistent calculation of the spectral and kinetic properties of the coupled electron-hole-photon system for pump rates ranging from well below to well above the laser threshold. The carrier scattering processes which lead to optical dephasing and the many-body renormalization of the carrier dispersion (light induced gap) are treated microscopically at a consistant level. Rather than providing a detailed derivation of the microscopic equations we present the general results and discuss the physical significance of the various terms. The general nonequilibrium Green's function theory for a semiconductor is presented in Ref. [10] and is extended here for the case of a semiconductor laser. We use the simplest version of the general theory, i.e., we make the well-known random-phase approximation (RPA) generalized to the nonequilibrium carrier-photon system. Even though it can be an interesting aspect of the theory, we ignore in a first step all interband Coulomb effects since their inclusion would considerably increase the complexity of our analysis. Screening is considered on a single-particle level and the renormalization and damping effects are computed in a microscopically consistent fashion. These more formal aspects of the theory will be presented in a forthcoming publication.

In this paper we start our analysis in Sec. II by describing the kinetic equations for a short-cavity semiconductor laser in a homogeneous and stationary situation. We analyze the carrier-carrier Coulomb scattering by numerically computing the electron/hole self-energies from the carrier Boltzmann equation. We extract the intraband relaxation and dephasing rates as functions of particle momentum k and establish the relation to optical dephasing. We verify that the relaxation time approximation for the carrier kinetics in semiconductor lasers is applicable as long as the scattering rates are computed consistently from the many-body formalism.

The detailed shape of the gain/absorption spectrum in the running short-cavity laser is determined by the competition between stimulated emission at the laser frequency and the carrier-carrier scattering. The probe gain spectrum depends sensitively on the inversion of carriers, i.e., on the carrier kinetics. To obtain the gain spectra we solve the coupled microscopic equations for the carrier inversion and for the spectral shape of the emitted light intensity.

In Sec. III we discuss the numerical evaluation scheme for our system of integral equations. Results are presented in Sec. IV for the example of a continuously pumped single-mode short-cavity GaAs laser. We show that a spectral hole develops around the frequency of the run-

 ©1992 The American Physical Society

ning laser mode, as soon as the laser is pumped above threshold. For the highest carrier densities investigated we find a substructure in the spectral hole which corresponds to the light-induced renormalization in the carrier dispersions. For above threshold carrier densities our calculations yield a high degree of gain saturation, i.e., compensation of loss and gain at the laser resonance.

II. KINETIC EQUATIONS

We consider the distribution function $f_c(k)$ of electrons in the conduction band of a semiconductor laser. In the spatially homogeneous case the kinetic equation can be written as

$$\left[\frac{\partial f_c(k)}{\partial t}\right]=\left[\frac{\partial f_c(k)}{\partial t}\right]_{\text{coll}}+\left[\frac{\partial f_c(k)}{\partial t}\right]_{\text{stim}}+\left[\frac{\partial f_c(k)}{\partial t}\right]_{\text{spont}}+\left[\frac{\partial f_c(k)}{\partial t}\right]_{\text{pump}}. \quad (2.1)$$

The corresponding equation for the valence-band electron distribution $f_v(k)$ is obtained by replacing c through v. The different terms on the right-hand side (rhs) of Eq. (2.1) describe the kinetic changes due to intraband carrier-carrier collision, stimulated emission of light, spontaneous emission, and pumping of electrons from the valence band into the conduction band, respectively.

For the purposes of this paper we do not need the detailed form of the pump rate. It is only included in Eq. (2.1) to balance the rate of change of the total number of carriers $N=2\sum_{\mathbf{k}} f_c(k)$. We denote the total pump rate P as

$$P=2\sum_{\mathbf{k}}\left[\frac{\partial f_c(k)}{\partial t}\right]_{\text{pump}}. \quad (2.2)$$

A. Carrier-carrier collisions

The expression for the carrier-carrier collision rate is

$$\left[\frac{\partial f_e(k)}{\partial t}\right]_{\text{coll}}=\Gamma_{\text{in}}^{e}[1-f_e(k)]-\Gamma_{\text{out}}^{e} f_e(k), \quad (2.3)$$

where the relaxation rates Γ_{in} and Γ_{out} describe carrier-carrier scattering due to Coulomb interaction. In RPA, these relaxation rates are given as [11]

$$\Gamma_{\text{in}}^{e}(\mathbf{k}_1)=\frac{2\pi}{\hbar}\sum_{\alpha,\mathbf{k}_2,\mathbf{k}_3,\mathbf{k}_4} 2|W(\mathbf{k}_2-\mathbf{k}_1)|^2 f_e(k_2)[1-f_\alpha(k_3)]f_\alpha(k_4)\delta_{\mathbf{k}_1+\mathbf{k}_3,\mathbf{k}_2,\mathbf{k}_4}\delta(\varepsilon_e(k_1)-\varepsilon_e(k_2)+\varepsilon_\alpha(k_3)-\varepsilon_\alpha(k_4)) \quad (2.4)$$

and

$$\Gamma_{\text{out}}^{e}(\mathbf{k}_1)=\frac{2\pi}{\hbar}\sum_{\alpha,\mathbf{k}_2,\mathbf{k}_3,\mathbf{k}_4} 2|W(\mathbf{k}_2-\mathbf{k}_1)|^2 [1-f_e(k_2)]f_\alpha(k_3)[1-f_\alpha(k_4)]\delta_{\mathbf{k}_1+\mathbf{k}_3,\mathbf{k}_2+\mathbf{k}_4}\delta(\varepsilon_e(k_1)-\varepsilon_e(k_2)+\varepsilon_\alpha(k_3)-\varepsilon_\alpha(k_4)), \quad (2.5)$$

where $W(k)$ is the screened Coulomb potential. For simplicity of notation we write Eqs. (2.4) and (2.5) in the electron-hole notation, where $f_e=f_c$ and $f_h=1-f_v$, and the summation index α runs over the indices e,h. ε_α denotes the single-particle energy of electrons or holes. The corresponding equation for the hole scattering rates is obtained from Eqs. (2.4) and (2.5) simply by substituting the index e by h.

A close inspection of Eqs. (2.3)–(2.5) shows that

$$\sum_{\mathbf{k}}\left[\frac{\partial f_c(k)}{\partial t}\right]_{\text{coll}}\equiv 0, \quad (2.6)$$

expressing the fact that carrier-carrier intraband scattering leads to redistribution of carriers within each band, without any interband transitions.

It is well know that the evaluation of the scattering rates in general requires a quite considerable numerical effort. However, for a situation not too far away from thermodynamic quasiequilibrium, we can approximate the collision by

$$\left[\frac{\partial f_c(k)}{\partial t}\right]_{\text{coll}}=-\frac{f_c(k)-f_c^F(k)}{\tau_c(k_0)}, \quad (2.7)$$

where

$$\frac{1}{\tau_c(k_0)}=\Gamma_{\text{in},0}^{c}(k_0)+\Gamma_{\text{out},0}^{c}(k_0) \quad (2.8)$$

and k_0 is a representative wave number at which the collision rates are evaluated. In this paper we chose the wave number k_0 corresponding to the laser frequency ω_0 (see Sec. IV). In Eq. (2.7) $f_c^F(k)$ denotes the electron quasiequilibrium Fermi distribution function and the index 0 on Γ indicates that the actual distribution function in Eqs. (2.4) and (2.5) have been replaced by $f_c^F(k)$. Furthermore, we used the fact that for $f_c(k)\equiv f_c^F(k)$, the total collision term Eq. (2.3) vanishes identically.

As discussed in detail in Ref. [11], the *relaxation time approximation* Eq. (2.7) is reasonable as long as the overall actual distribution function deviates only weakly from a Fermi function, even though the deviations in some small range of k values may be relatively significant. Generally, the overall deviation has to satisfy the condition

$$\sum_{\mathbf{k}}|f_c(k)-f_c^F(k)| \ll \sum_{\mathbf{k}} f_c(k), \quad (2.9)$$

which is well fulfilled for the presently studied case of a

single-mode semiconductor laser where the running laser mode leads to changes of the carrier distributions which are centered around the k value of the mode.

B. Stimulated and spontaneous emission

The stimulated and spontaneous emission rates in Eq. (2.1) are given by

$$\left[\frac{\partial f_c(k)}{\partial t}\right]_{\text{stim}} = -[f_c(k)-f_v(k)] \times \frac{1}{2\pi}\int d\omega\, A_{cv}(k,\omega)\lambda_{\text{stim}}(\omega) \quad (2.10)$$

and

$$\left[\frac{\partial f_c(k)}{\partial t}\right]_{\text{spont}} = -f_c(k)[1-f_v(k)] \times \frac{1}{2\pi}\int d\omega\, A_{cv}(k,\omega)\lambda_{\text{spont}}(\omega) , \quad (2.11)$$

where A_{cv} is the interband carrier spectral function and λ is the photon function. These quantities are discussed below. The carrier population factors $[f_c(k)-f_v(k)]$ and $f_c(k)[1-f_v(k)]$ in Eqs. (2.10) and (2.11) are related through

$$[f_c(k)-f_v(k)] = f_c(k)[1-f_v(k)] - f_v(k)[1-f_c(k)] , \quad (2.12)$$

expressing the fact that the stimulated emission is proportional to the inversion $f_c(k)-f_v(k)$, which is the difference between spontaneous emission $\propto f_c(k)[1-f_v(k)]$ and absorption $\propto f_v(k)[1-f_c(k)]$.

In optical transitions in a semiconductor, the spectral function for the single-particle states $A_c(k\omega)$ and $A_v(k\omega)$ occur always in the form of a combined spectral function

$$A_{cv}(k,\omega) = -\frac{\hbar}{2\pi}\int d\omega'\, A_c(k,\omega-\omega')A_v(k,\omega') . \quad (2.13)$$

Since a detailed analysis of these spectral functions is presented in Ref. [10], we omit the discussion of these quantities in the present paper and give only the explicit form of A_{cv} in Sec. III.

In Eq. (2.10) the coupling of the semiconductor to the light field is described by the photon function

$$\lambda_{\text{stim}}(\omega) = \left[\frac{j_{cv}}{c}\right]^2 \frac{1}{V}\sum_{\mathbf{q}} f_{\text{ph}}(\mathbf{q},\omega) , \quad (2.14)$$

where j_{cv} is the interband current matrix element. Similarly, the function $\lambda_{\text{spont}}(\omega)$ in Eq. (2.11) is given as

$$\lambda_{\text{spont}}(\omega) = \left[\frac{j_{cv}}{c}\right]^2 \frac{1}{V}\sum_{\mathbf{q}} A_{\text{ph}}(\mathbf{q},\omega) . \quad (2.15)$$

The photon spectral function A_{ph} and the photon distribution $f_{\text{ph}}(q,\omega)$ enter into Eqs. (2.14) and (2.15) since the light field is described in complete analogy to the material quantities. The photon distribution function is the Fourier transform of the field-correlation function $\langle A(r_1t_1)A(r_2t_2)\rangle$ into k space with respect to r_1-r_2 and into ω space with respect to t_1-t_2, respectively. The photon spectral function is the corresponding retarded expression constructed form the field-correlation function. Because of damping, i.e., broadening of the photon states, the spectral function of the photons does not simply consist of δ functions peaked at the renormalized dispersion $q(\omega)$, but is given by

$$A_{\text{ph}}(\mathbf{q},\omega) = \frac{\gamma_{\text{ph}}}{[q^2-q^2(\omega)]^2+\gamma_{\text{ph}}^2} . \quad (2.16)$$

Here γ_{ph} denotes the photon damping and is in a laser the difference between the background losses $2\kappa(\omega)$ and the optical gain $G(\omega)$:

$$\gamma_{\text{ph}}(\omega) = 2\kappa(\omega) - G(\omega) . \quad (2.17)$$

Since we investigate a short-cavity semiconductor laser, where only one cavity mode exists within the gain bandwidth, we model the resonator losses as

$$\kappa(\omega) = \begin{cases} \infty & \text{for } \omega\neq\omega_0 \\ \kappa_0 & \text{otherwise} . \end{cases} \quad (2.18)$$

Note, that for stationary operation conditions

$$\gamma_{\text{ph}}(\omega) > 0 \quad (2.19)$$

must be always fulfilled; otherwise the retarded photon Green's function $D^{\text{ret}}(\mathbf{q},t)$ would diverge for $t\to\infty$.

Equation (2.14) shows that the stimulated emission with the optical frequency ω is proportional to $\sum_{\mathbf{q}} f_{\text{ph}}(\mathbf{q},\omega)$, i.e., the total number of photons with frequency ω. We see from Eq. (2.15) that the spontaneous emission of course needs no real occupation of photons. It involves only the spectral functions of the photons and of the semiconductor to assure energy conservation in the transition.

As a consequence of the broadening γ_{ph}, photons with given momentum can contribute to various energetic transitions in the semiconductor. We therefore need the spectral resolution of the occupation function $f_{\text{ph}}(\mathbf{q},\omega)$ for a given mode $\mathbf{q}$, which yields the information of the distribution of the occupation of the mode $\mathbf{q}$ with frequency ω. This is in contrast to the carrier distribution functions, where we are only interested in the total occupations of the $\mathbf{k}$ states, which are determined by the frequency-integrated distribution functions.

The function $\lambda_{\text{stim}}(\omega)$ determines the spectral shape of the stimulated emitted light as

$$I_{\text{stim}}(\omega) = \frac{\omega^2}{c}\left[\frac{c}{j_{cv}}\right]^2 \hbar\lambda_{\text{stim}}(\omega) . \quad (2.20)$$

Correspondingly I_{spont} follows from λ_{spont}.

The photon distribution function obeys an equation which is formally very similar to the carrier Boltzmann equation (2.3). The analogy to in and out scattering of carriers due to Coulomb scattering is the emission and

absorption of photons due to electron-hole-pair creation and annihilation. The photon Boltzmann equation is discussed in Ref. [10] as Eq. (4.20). It involves the time derivative of f_{ph} with respect to the center-of-mass time $(t_1+t_2)/2$ and analogous spatial derivatives. In the following, we restrict ourselves to homogeneous systems in both space and time. This allows a simple solution of the photon Boltzman equation, as we only have to make the emission and absorption contributions equal. Using the explicit form Eq. (2.16) for the spectral function of the photons yields

$$f_{ph}(\mathbf{q},\omega)=\frac{\Gamma_{in}^{ph}(\omega)}{[q^2-q^2(\omega)]^2+\gamma_{ph}^2(\omega)}\ , \tag{2.21}$$

where $\Gamma_{in}^{ph}(\omega)$ is proportional to the scattering rate into a photon mode

$$\Gamma_{in}^{ph}(\omega)=\left[\frac{j_{cv}}{c}\right]^2\frac{2}{V}\sum_k A_{cv}(k,\omega)f_c(k)[1-f_v(k)]\ . \tag{2.22}$$

Note that the weak dependence on the photon wave vector has been neglected here.

Finally, we have to give the explicit form of the gain function $G(\omega)$ that enters the photon damping γ_{ph}. Within the random-phase approximation, $G(\omega)$ can be written as

$$G(\omega)=\left[\frac{j_{cv}}{c}\right]^2\frac{2}{V}\sum_k A_{cv}(k,\omega)[f_c(k)-f_v(k)]\ . \tag{2.23}$$

For given spectral functions A_c, A_v, and A_{ph} we have now a closed set of nonlinear equations of the distributions functions f_c, f_v, and f_{ph}.

III. NUMERICAL EVALUATION

As a simple numerical example we evaluate our equations for the case of a short-cavity bulk GaAs semiconductor laser of resonator length L, where only one resonator mode exists within the spectral region of optical gain. To obtain the stimulated emission spectrum, we have to evaluate the $\mathbf{q}$ summation in Eq. (2.14). Taking an output beam of diameter d, we assume that only modes within an angle of $d/L \ll 1$ contribute to the emission. Hence we approximate

$$f_{ph}(\mathbf{q},\omega)=\begin{cases} f_{ph}(q_z,\omega) & \text{for } q_\perp<\frac{d}{L}q_z \\ 0 & \text{otherwise}\end{cases} \tag{3.1}$$

allowing us to evaluate the integration over the perpendicular part of the wave vector $q_\perp$ in the q integration of Eq. (2.14):

$$\int d^3q f_{ph}(\mathbf{q},\omega)=\pi\left[\frac{d}{2L}\right]^2\int dq_z q_z^2 f_{ph}(q_z,\omega)\ . \tag{3.2}$$

We then obtain form (2.14) with (2.21),

$$\lambda_{stim}(\omega)=-\left[\frac{j_{cv}}{c}\right]^2\frac{1}{16\pi}\left[\frac{d}{2L}\right]^2\tilde{q}(\omega)\frac{\Gamma_{in}^{ph}(\omega)}{\gamma_{ph}(\omega)}\ , \tag{3.3}$$

where the damping of the photon states formally leads to a further renormalization of the renormalized photon dispersion:

$$\tilde{q}(\omega)=\sqrt{[q^2(\omega)+[q^4(\omega)+\gamma_{ph}^2(\omega)]^{1/2}]/2}\ . \tag{3.4}$$

In the vicinity of the laser mode ω_0 the damping approaches zero so that in that spectral region $\tilde{q}(\omega)\simeq q(\omega)$. For simplicity we completely ignore the renormalizations of the photon dispersion in our numerical evaluations, approximating $\tilde{q}(\omega)\simeq\omega/c$.

Since we are dealing with a configuration that allows only single-mode operation, essentially only a small region around the laser frequency ω_0 contributes to the stimulated emission. Furthermore, it is well known [1–3] that the linewidth of a semiconductor laser is small in comparison to the broadening which is predominantly determined by the fast dephasing processes due to Coulomb interaction. Therefore, we evaluate $A_{cv}(k,\omega)$ at the laser frequency ω_0 and approximate in Eq. (2.10).

$$\begin{aligned}\frac{1}{2\pi}&\int d\omega\, A_{cv}(k,\omega)\lambda_{stim}(\omega)\\ &\simeq A_{cv}(k,\omega_0)\frac{1}{2\pi}\int d\omega\,\lambda_{stim}(\omega)\\ &\equiv A_{cv}(k,\omega_0)\lambda_0\ ,\end{aligned} \tag{3.5}$$

where λ_0 and $\Gamma_{in}^{ph}(\omega)$ have to be computed self-consistently to satisfy Eq. (3.3). The quantity λ_0 is related to the square of the Rabi frequency [10]

$$\Omega_R^2=\frac{2\pi}{\hbar}\lambda_0\ . \tag{3.6}$$

It is a good approximation to assume that the spontaneous emission rate is spectrally broad and does not significantly influence the spectral properties near the resonances. Integrating Eq. (2.1) over $\mathbf{k}$ and making use of the fact that the intraband collisions do not change the total number of the carriers in the bands, we get

$$P+\left[\frac{\partial N}{\partial t}\right]_{stim}+\left[\frac{\partial N}{\partial t}\right]_{spont}=0\ . \tag{3.7}$$

For our evaluations we ignore the frequency dependence of P and $(\partial N/\partial t)_{spont}$ and use these quantities as parameters.

As has been discussed [10,12,13] for a passive semiconductor excited with a monochromatic field, laser induced bands and a renormalization of the electron dispersion appear which lead to a modification in the spectral shape of the interband transition rates near the resonance. This leads to an interband spectral function of the form [10]

$$\begin{aligned}A_{cv}(k\omega)=4\pi^2[&a^2(k)\delta_\gamma(\hbar\omega-E_{cv}(k))\\ &+b^2(k)\delta_\gamma(\hbar\omega+E_{cv}(k)-2\hbar\omega_0)\\ &+2a(k)b(k)\delta_\gamma(\hbar\omega-\hbar\omega_0)]\ ,\end{aligned} \tag{3.8}$$

where δ_γ is a broadened delta function. The damping

$$2\gamma(k)=\frac{1}{\tau_c(k)}+\frac{1}{\tau_v(k)} \tag{3.9}$$

is the sum of the relaxation rates (2.8) resulting from carrier-carrier collisions. The three terms in Eq. (3.8) result from transitions between the "dressed" semiconductor bands [12,10], which include the light induced splitting of the conduction and valence bands. The factors $a(k),b(k)$ and the renormalized dispersion $E_{cv}=E_c-E_v$ are discussed in Eqs. (3.8), (3.15), and (3.17) of Ref. [10] and will not be repeated here. It is only important to note at this point that the band renormalization is a function of the field intensity, through λ_0, and disappears for weak fields, leaving the usual semiconductor band structure. Because of this field intensity dependence it is not crucial for the band renormalization whether one assumes a situation where $\langle A\rangle\neq 0$, as in Ref. [10], or $\langle A\rangle=0$ as in the present case of a semiconductor laser.

For the numerical analysis we choose a laser frequency ω_0 close to the gain maximum at threshold. In a realistic short-cavity semiconductor laser this frequency is determined by details of the experimental configuration such as the cavity length. Assuming a carrier density, which is implicitly determined by the pump rate, we compute the chemical potentials entering the quasiequilibrium distributions of the carriers in the conduction and valence bands. Inserting Eq. (3.5) into Eq. (2.10), and then Eqs. (2.10) and (2.7) into Eq. (2.1) yields in steady state

$$\frac{f_c(k)-f_c^F(k)}{\tau_c}=[f_v(k)-f_c(k)]A_{cv}(k,\omega_0)\lambda_0 - \frac{f_c(k)[1-f_v(k)]}{\tau_{\rm spont}}\ , \tag{3.10}$$

where the pump contribution enters implicitly through the chemical potential in f^F, and

$$\frac{1}{\tau_{\rm spont}}\equiv\int d\omega\, A_{cv}(k,\omega)\lambda_{\rm spont}(\omega)\ . \tag{3.11}$$

In Eq. (3.11) the weak k dependence has been ignored. An equation analogous to (3.10) is valid for the electron distribution in the valence band, where except for a sign change all terms on the rhs are identical to (3.10), so that

$$\frac{f_c(k)-f_c^F(k)}{\tau_c}=-\frac{f_v(k)-f_v^F(k)}{\tau_v}\ . \tag{3.12}$$

This equation shows that the ratio of the deviations from thermal distributions in the different bands, i.e., the ratio of the kinetic holes, is inversely proportional to the ratio of the relaxation times in these bands.

We solve Eqs. (3.10) and (3.12) by eliminating f_v, which results in a quadratic equation for the carrier distributions as functions of λ_0. Using Eq. (3.3) with (2.22), (2.17), and (2.23) we then compute $\lambda_{\rm stim}(\omega)$, which depends on λ_0 via the carrier distributions. After obtaining a self-consistent solution, we then calculate the total **k**-integrated emission rates, and from these, using Eq. (3.7), we determine the pump rate required for the assumed steady state.

IV. RESULTS AND DISCUSSION

In order to study the semiconductor laser situation we first have to evaluate the carrier scattering and dephasing rates for the relevant carrier densities. To this end we numerically solve the full equations (2.3)–(2.5) for the case in which equilibrium electron and hole distribution functions have been distorted at small k values to study the relaxation of a kinetic hole in a high-density carrier distribution [11]. Figure 1(a) shows the electron and hole distributions at various times after the initialization. We

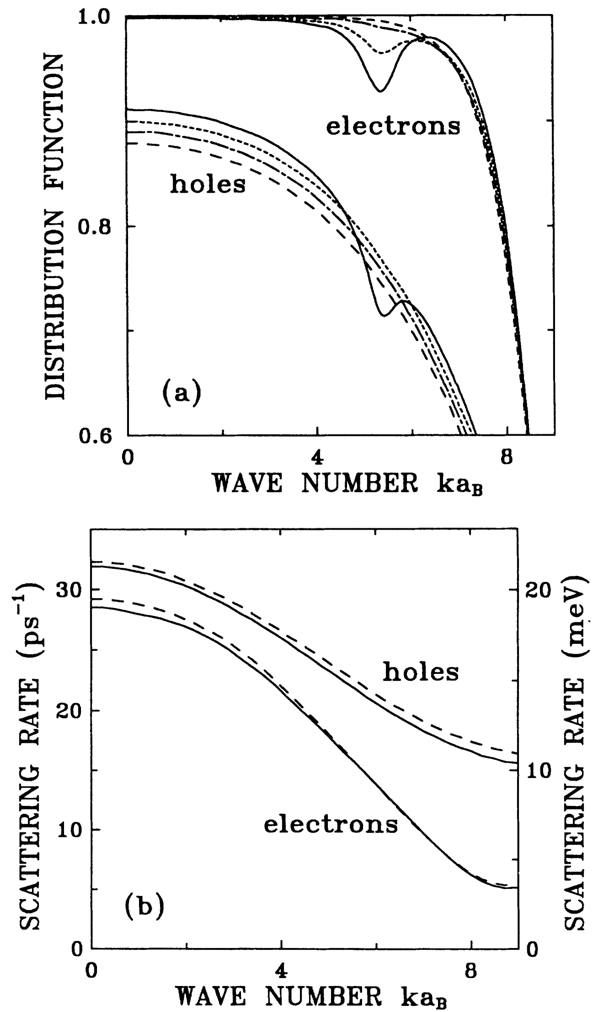

FIG. 1. Relaxation of initially disturbed Fermi distribution functions for a density $n=8\times10^{18}$ cm^{-3} and a temperature $T\simeq300$ K. Shown are the distribution functions of electrons and holes (a) and the corresponding total scattering rates (b) as a function of the carrier momentum in units of a_B where $a_B=140$ Å. The initial ($t=0$) distribution functions are the solid lines and the consecutive times are $t=60$ fs (short-dashed line), $t=200$ fs (dash-dotted line), and the final time $t=1.1$ ps (long-dashed line). The corresponding total scattering rates are shown only for the initial and final times.

see that under the influence of carrier-carrier collisions the kinetic hole vanishes on the time scale of $\simeq 50$ fs. Figure 1(b) shows that the scattering rates

$$\Gamma^{\alpha}(k)=\Gamma_{\rm in}^{\alpha}(k)+\Gamma_{\rm out}^{\alpha}(k),\quad \alpha=e,h \tag{4.1}$$

are almost time independent and, as discussed in Ref. [11], a relaxation time approximation seems justified.

Taking the computed scattering and dephasing rates in the relaxation time approximation, we can now solve the full set of laser equations. For simplicity, we investigate a short-cavity semiconductor laser which has only one cavity mode in the gain region. Hence, we arbitrarily choose a laser frequency ω_0, which we keep fixed in our calculations, i.e., we neglect mode pulling effects which would lead to small shifts of the actual laser frequency for different operation conditions. We use the relaxation and dephasing rates at the wave number k_0 corresponding to ω_0. Our numerical scheme yields the self-consistent solutions for the carrier distribution functions, the gain profile, and the laser output.

In Figs. (2) and (3) we show examples of the steady-state solutions for different carrier densities, i.e., different injection pump rates. For illustration we show in Figs. 2(a) and 2(b) the carrier distributions and the corresponding gain spectra for a threshold carrier density of 8×10^{18} cm^{-3} and various field strengths (Rabi frequencies). As we can see in Fig. 2(b) for small Rabi frequencies the gain at the laser frequency ω_0 is below the loss $2\kappa_0$, so that no laser emission occurs. Hence, the corresponding distribution functions in Fig. 2(a) are basically the thermal quasiequilibrium distributions. When $G(\omega_0)$ approaches $2\kappa_0$, laser action sets in. Above-threshold kinetic holes in the distribution functions emerge at the resonance energy. The width of these holes is essentially determined by the carrier-carrier scattering rates, hence it is in general large in comparison to the spectral width of the Fabry-Pérot resonance.

Simultaneously with the occurrence of the kinetic holes, the optical gain develops a spectral hole whose width is determined by the dephasing rate, see Fig. 2(b). For large field strengths substructures in the spectral hole appear which result from light induced renormalizations of the band structure. They lead to gain depletion in the spectral region $\pm\Omega_R$ around ω_0. The light induced bandstructure renormalization corresponds to the optical Stark splitting (dynamic Stark effect) of the various k states around the laser resonance. Since we do not spectrally resolve the carrier distribution for given k, these substructures do not show up in Fig. 2(a).

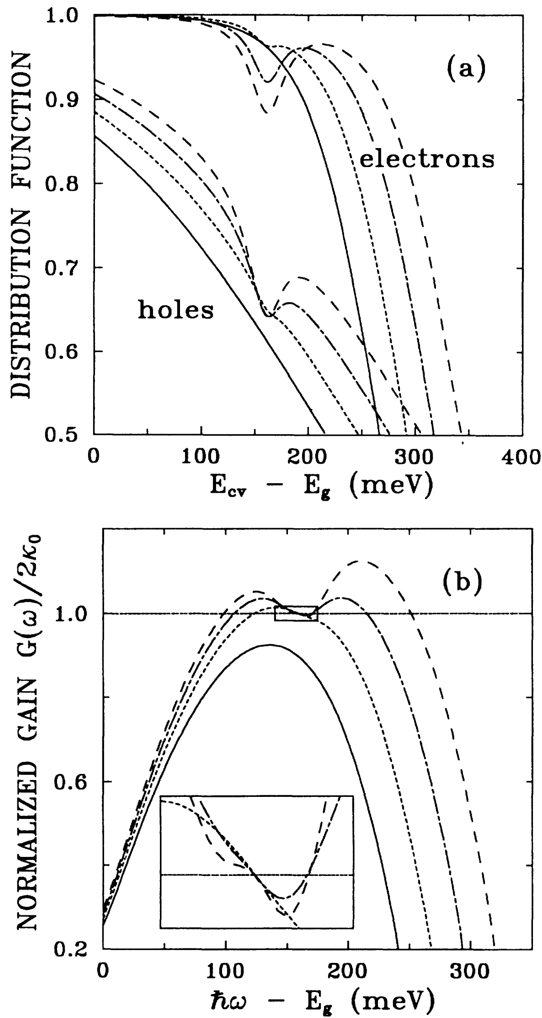

FIG. 2. (a) Room-temperature electron and hole distributions functions for a short-cavity GaAs laser which supports a single lasing mode. The threshold carrier density is 8×10^{18} cm^{-3}. (b) Gain spectra corresponding to the carrier distributions of (a). The dephasing rates have been obtained from the results of Fig. 1. The gain is plotted in units of the total losses $2\kappa_0$ of the laser mode. The different curves are computed for the Rabi energies $\hbar\Omega_R$ (in 10^{-6} meV): 9.9 (solid line), 13 (short-dashed line), 28 (dash-dotted line), and 37 (long-dashed line). The inset to (b) is an enlargement of the gain spectra around the laser frequency.

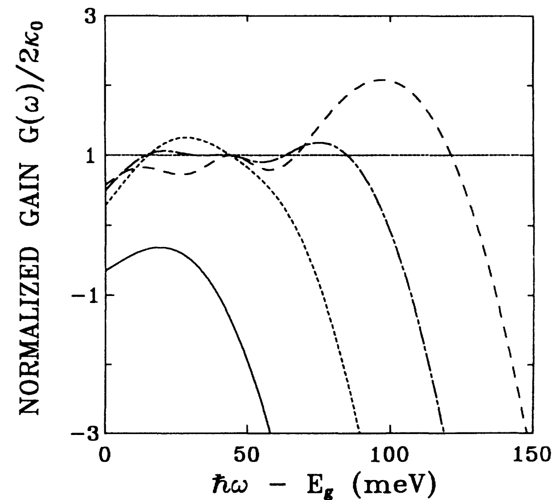

FIG. 3. Room-temperature gain spectra for the threshold carrier density of 2×10^{18} cm^{-3}. The different curves are computed for the Rabi energies $\hbar\Omega_R$ (in 10^{-6} meV): 4.7 (solid line), 45 (short-dashed line), 94 (dash-dotted line), and 132 (long-dashed line).

To investigate the parameter dependence of the spectral holes, we show in Fig. 3 computed gain spectra for the lower threshold carrier density of 2×10^{18} cm^{-3} corresponding to decreased resonator losses. As in Fig. 2(b), we see in Fig. 3 the development of a spectral hole when the laser is pumped above threshold. Also, the substructures due to Rabi splitting develop for sufficiently high field strengths.

The comparison of the calculations for different threshold carrier densities shows that hole burning is easier to observe at higher threshold carrier densities, simply because the gain region is spectrally broader. Even though spectral holes occur already for Rabi frequencies lower than the dephasing rate, the band-splitting related substructures inside the spectral hole are resolved only when

$$\Omega_R \geq \gamma(k_0) \ . \tag{4.2}$$

To study the onset of laser action as a function of carrier density we plot in Fig. 4 the net photon losses Eq. (2.17) at ω_0 for different pump rates. We observe a strong compensation of gain and background losses at resonance when the carrier density changes from $N_{\text{threshold}}$ to slightly above $N_{\text{threshold}}$. At still larger pump rates the mode quickly saturates.

In summary, we present a microscopically consistent theory for the spectral and kinetic properties of the coupled electron-hole-photon system in a short-cavity semiconductor laser. We evaluate the theory for the simplified case where the interband electron-hole Coulomb effects are neglected. We observe the development of kinetic holes, which are holes in the electron and hole distribution functions, and of a spectral hole, i.e., a hole in the gain spectrum of a running laser. At not too high intensities the occurrence of a spectral hole is predominantly a consequence of the kinetic hole, i.e., of the carrier depletion at the frequency of the running laser mode. At higher laser field strengths also light-induced renormalizations of the carrier dispersions become important leading to substructures within the spectral hole. The carrier dephasing is crucial for the details of the spectral and kinetic holes, see Eq. (4.2). The nonequilibrium shape of the carrier distributions causes a nonlinear gain saturation, i.e., compensation between gain and loss up to seven orders of magnitude within a small range of pump rates at and slightly above the threshold pump rate.

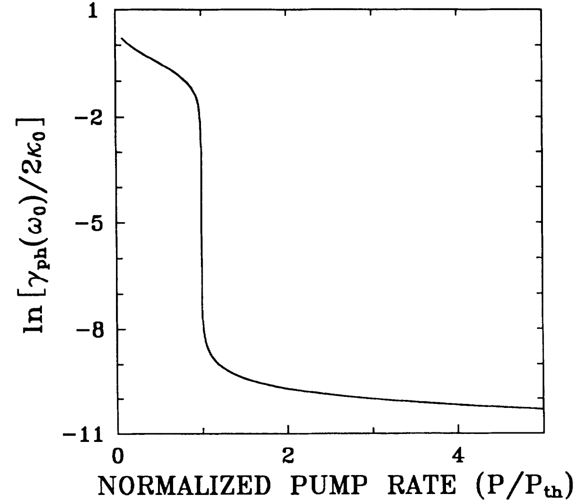

FIG. 4. Logarithmic plot of the net photon loss rate, Eq. (2.17), at the laser frequency ω_0 in units of the losses $2\kappa_0$ at the laser frequency ω_0 vs normalized pump rate. P_{th} is the threshold pump rate.

ACKNOWLEDGMENTS

The Universität Rostock part of this work has been supported by the Volkswagenstiftung, Forschungsanlage KFA Jülich and the Deutsche Forschungsgemeinschaft. The University of Arizona part of this work was supported through grants from the NSF, ARO/AFOSR (JSOP), NATO, the Optical Circuitry Cooperative of the University of Arizona, and through a grant for CPU time at the Pittsburgh Supercomputer Center. R.B. thanks the DFG (Deutsche Forschungsgemeinschaft, Federal Republic of Germany) for financial support. D.S. acknowledges the support of the U.S. Department of Education through the Physics Department.

[1] A. Yariv, *Optical Electronics*, 3rd ed. (Holt, Rinehart and Winston, New York, 1985).
[2] G. P. Agarwal and N. K. Dutta, *Long-Wavelength Semiconductor Lasers* (Van Nostrand Reinhold, New York, 1986).
[3] G. H. B. Thompson, *Physics of Semiconductor Laser Devices* (Wiley, Chichester, 1980).
[4] V. Korenman, Ann. Phys **39**, 72 (1966).
[5] B. Zée, IEEE J. Quantum Electron. **QE-14**, 727 (1978).
[6] N. B. Patel, P. Brosson, and J. E. Ripper, App. Phys. Lett **34**, 330 (1979).
[7] D. Kasemset and C. G. Fonstad, IEEE, J. Quantum Electron. **QE-18**, 1078 (1982).
[8] R. Frankenberger and R. Schimpe, Appl. Phys. Lett. **57**, 2520 (1990).
[9] M. P. Kessler and E. Ippen, Appl. Phys. Lett. **51**, 1765 (1987); K. L. Hall, J. Mark, E. P. Ippen, and G. Eisenstein, *ibid.* **56**, 1740 (1990).
[10] K. Henneberger and H. Haug, Phys. Rev. B **38**, 9759 (1988).
[11] R. Binder, D. Scott, A. E. Paul, M. Lindberg, K. Henneberger, and S. W. Koch, Phys. Rev. B (to be published).
[12] V. F. Elesin, Zh. Eksp. Teor. Fiz. **59**, 602 (1970) [Sov. Phys.—JETP **32**, 328 (1971)].
[13] K. Henneberger and K. H. Kühn, Physica **A150**, 439 (1988).